Supporting information(SI)

Combining Potassium With Positive Oxygen-balanced Polynitropyrazole: a Promising Way to Develop Green Primary Explosives.

Benyue Guo[a,1], Xiya Zhang[a,1], Xiangyang Lin*[a], Haifeng Huang*[b], Jun Yang*[b]

[a] School of Chemical Engineering, Nanjing University of Science and Technology, Xiaolingwei 200, Nanjing, Jiangsu, China. E-mail: lingxiangyang@njust.edu.cn;

[b] CAS Key Laboratory of Energy Regulation Materials, Center for Excellent in Molecular Synthesis, Shanghai institute of Organic Chemistry, University of Chinese Academy of Sciences, Chinese Academy of Sciences, Shanghai 200032, (PR China).

E-mail: yangj@sioc.an.cn, hfhuang@sioc.ac.cn

1. Experimental section

^{1}H and ^{13}C NMR spectra were recorded on 500 MHz (Bruker AVANCE 500) nuclear magnetic resonance spectrometers operating at 500 and 125 MHz, respectively, Chemical shifts in ^{1}H and ^{13}C NMR spectra are reported relative to DMSO. The decomposition points were recorded on a METTLER TOLEDO DSC823E equipment at a heating rate of 10 °C min^{-1} in closed Al containers with a nitrogen flow of 25 ml min^{-1}. FT-IR spectra were analyzed with the NicoLiteS10(Thermal Fisher, USA) FT-IR. Friction sensitivity, impact sensitivity of samples were measured by using the standard BAM methods. Elemental analyses were performed on an Elementar Vario MICRO cube (Germany) elemental analyzer.

X-ray crystallography

X-ray of all single crystals were carried out at 140K or 170k on a Bruker D8 VENTURE diffractometer using Mo-Kα radiation (λ=0.71073Å). Integration and scaling of intensity data was performed using the SAINT program. Data were corrected for the effects of absorption using SADABS[1]. The structures were solved by direct method and refined with full-matrix least-squares technique using SHELX-2014[2] software. Non-hydrogen atoms were refined with anisotropic displacement parameters, and hydrogen atoms were places in calculated positions and refined with riding model.

2. Crystallographic data for compound 6 and 8·2H₂O

(a1)

(a2)

(b1)

(b2)
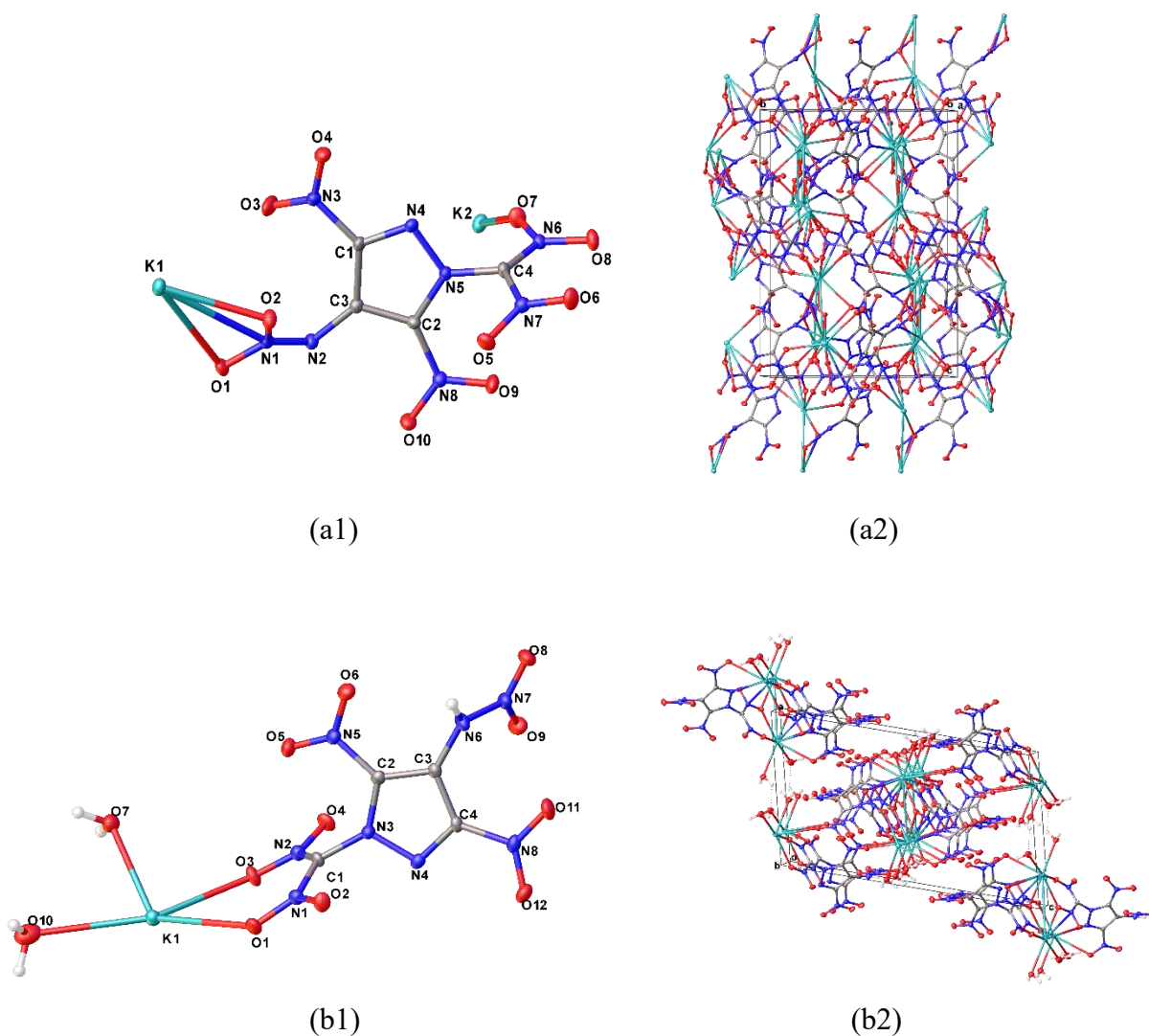
Figure S1: (a1) (b1): Displacement ellipsoid plot (30%) of compounds **6** and **8**·2H₂O; (a2) (b2): Ball-and-stick packing diagram of compounds **6** and **8**·2H₂O viewed down the a-axis and b-axis, respectively. The dashed lines indicate hydrogen bonding.

Table S1. Crystal data and structure refinement for compound **6** and **8·2H₂O**.

Compound	**6**	**8·2H₂O**
CCDC	CCDC-2081188	CCDC-2098704
Empirical formula	$C_4K_2N_8O_{10}$	$C_4H_5KN_8O_{12}$
Formula weight	398.32	396.26
Temperature/K	170.0	140.0
Crystal system	orthorhombic	monoclinic
Space group	Pbca	P2₁/n
Unit cell dimensions	a=10.7902(3)Å b=12.9624(4)Å c=17.9460(6)Å α=90° β=90° γ=90°	a=11.266(6)Å b=6.3213(19)Å c=19.213(7)Å α=90° β=103.155(17)° γ=90°
Volume/Å³	2510.05(13)	1332.4(9)
Z	8	4
ρ_{calc} g/cm³	2.108	1.975
Crystal size/mm³	0.12 × 0.11 × 0.06	0.11 × 0.06 × 0.03
Radiation	MoKα (λ = 0.71073)	MoKα (λ = 0.71073)
2Θ range for data collection/°	4.54 to 52.772	3.852 to 52.802
Index ranges	-13 ≤ h ≤ 13, -16 ≤ k ≤ 14, -22 ≤ l ≤ 20	–
Reflections collected	19689	2711
Independent reflections	2551 [R_{int} = 0.0555, R_{sigma} = 0.0307]	2711 [R_{int} = 0, R_{sigma} = 0.0826]
Data/restraints/parameters	2551/0/217	2711/0/228
Goodness-of-fit on F²	1.057	1.075
Final R indexes [I>=2σ (I)]	R_1 = 0.0285, wR_2 = 0.0627	R_1 = 0.0686, wR_2 = 0.1131
Final R indexes [all data]	R_1 = 0.0403, wR_2 = 0.0686	R_1 = 0.1183, wR_2 = 0.1311
Largest diff. peak/hole / e Å⁻³	0.28/-0.31	0.39/-0.40

Table S2. Bonds Lengths of **6**

Atom	Atom	Length/Å	Atom	Atom	Length/Å
K(1)	K(2)	4.4451(6)	O(8)	N(6)	1.253(2)
K(1)	K(2)	4.1700(6)	O(4)	N(3)	1.230(2)
K(1)	O(2)	2.7055(14)	O(1)	N(1)	1.257(2)
K(1)	O(8)	2.7981(14)	O(7)	N(6)	1.249(2)
K(1)	O(4)	2.9564(15)	O(10)	N(8)	1.230(2)
K(1)	O(1)	2.9977(15)	O(9)	N(8)	1.231(2)
K(1)	O(10)	2.7727(15)	O(5)	N(7)	1.246(2)
K(1)	O(5)	2.7812(14)	O(6)	N(7)	1.238(2)
K(1)	N(1)	3.2097(16)	N(1)	N(2)	1.308(2)
K(1)	N(4)	2.8371(16)	N(6)	C(4)	1.365(2)
K(1)	N(2)	3.0648(16)	O(3)	N(3)	1.221(2)
K(2)	O(2)	2.6417(14)	N(4)	N(5)	1.343(2)
K(2)	O(8)	2.7380(14)	N(4)	C(1)	1.316(2)
K(2)	O(4)	3.0086(15)	N(2)	C(3)	1.386(2)
K(2)	O(1)1	2.6570(14)	N(5)	C(4)	1.401(2)
K(2)	O(7)	2.6359(14)	N(5)	C(2)	1.379(2)
K(2)	O(10)	3.1737(16)	N(7)	C(4)	1.397(2)
K(2)	O(9)	2.8650(15)	N(8)	C(2)	1.423(2)
K(2)	O(6)	2.7294(16)	N(3)	C(1)	1.447(2)
K(2)	N(8)	3.3504(17)	C(1)	C(3)	1.423(3)
O(2)	N(1)	1.2652(19)	C(3)	C(2)	1.379(3)

Table S3. Bonds Angles for **6**

Atom	Atom	Atom	Angle/°	Atom	Atom	Atom	Angle/°
K(2)	K(1)	K(2)	108.23(12)	O(7)	K(2)	O(8)	120.94(5)
O(2)	K(1)	K(2)	38.21(3)	O(7)	K(2)	O(4)	105.46(4)
O(2)	K(1)	K(2)	75.41(3)	O(7)	K(2)	O(1)	163.82(5)
O(2)	K(1)	O(8)	97.58(4)	O(7)	K(2)	O(10)	65.21(4)
O(2)	K(1)	O(4)	75.40(4)	O(7)	K(2)	O(9)	86.16(5)
O(2)	K(1)	O(1)	44.44(4)	O(7)	K(2)	O(6)	97.03(5)
O(2)	K(1)	O(10)	118.55(4)	O(7)	K(2)	N(8)	78.79(4)
O(2)	K(1)	O(5)	142.60(4)	O(10)	K(2)	K(1)	166.65(3)
O(2)	K(1)	N(1)	22.71(4)	O(10)	K(2)	K(1)	89.52(3)
O(2)	K(1)	N(4)	124.51(5)	O(10)	K(2)	N(8)	21.52(4)
O(2)	K(1)	N(2)	79.54(4)	O(9)	K(2)	K(1)	130.40(3)
O(8)	K(1)	K(2)	36.13(3)	O(9)	K(2)	K(1)	75.09(3)
O(8)	K(1)	K(2)	135.74(3)	O(9)	K(2)	O(4)	85.34(4)
O(8)	K(1)	O(4)	143.11(4)	O(9)	K(2)	O(10)	41.71(4)
O(8)	K(1)	O(1)	69.09(4)	O(9)	K(2)	N(8)	21.05(4)
O(8)	K(1)	N(1)	78.93(4)	O(6)	K(2)	K(1)	102.71(3)
O(8)	K(1)	N(4)	136.31(5)	O(6)	K(2)	K(1)	79.97(3)

O(8)	K(1)	N(2)	124.49(4)	O(6)	K(2)	O(8)	57.92(4)
O(4)	K(1)	K(2)	108.76(3)	O(6)	K(2)	O(4)	144.77(4)
O(4)	K(1)	K(2)	46.16(3)	O(6)	K(2)	O(10)	89.14(4)
O(4)	K(1)	O(1)	82.09(4)	O(6)	K(2)	O(9)	123.48(4)
O(4)	K(1)	N(1)	83.32(4)	O(6)	K(2)	N(8)	104.43(4)
O(4)	K(1)	N(2)	90.38(4)	N(8)	K(2)	K(1)	151.40(3)
O(1)	K(1)	K(2)	72.84(3)	N(8)	K(2)	K(1)	77.68(3)
O(1)	K(1)	K(2)	35.54(3)	K(2)	O(2)	K(1)	102.49(4)
O(1)	K(1)	N(1)	23.04(4)	N(1)	O(2)	K(1)	101.65(10)
O(1)	K(1)	N(2)	123.66(4)	N(1)	O(2)	K(2)	135.58(11)
O(10)	K(1)	K(2)	112.08(3)	K(2)	O(8)	K(1)	106.81(5)
O(10)	K(1)	K(2)	120.43(3)	N(6)	O(8)	K(1)	127.53(10)
O(10)	K(1)	O(8)	76.51(4)	N(6)	O(8)	K(2)	125.65(10)
O(10)	K(1)	O(4)	138.98(4)	K(1)	O(4)	K(2)	88.70(4)
O(10)	K(1)	O(1)	136.18(4)	N(3)	O(4)	K(1)	122.24(11)
O(10)	K(1)	O(5)	93.62(4)	N(3)	O(4)	K(2)	111.14(11)
O(10)	K(1)	N(1)	125.23(4)	K(2)	O(1)	K(1)	103.48(5)
O(10)	K(1)	N(4)	91.11(5)	N(1)	O(1)	K(1)	87.99(10)
O(10)	K(1)	N(2)	58.45(4)	N(1)	O(1)	K(2)	128.87(11)
O(5)	K(1)	K(2	138.80(3)	N(6)	O(7)	K(2)	152.17(12)
O(5)	K(1)	K(2)	74.97(3)	K(1)	O(10)	K(2)	120.25(5)
O(5)	K(1)	O(8)	70.34(4)	N(8)	O(10)	K(1)	152.22(13)
O(5)	K(1)	O(4)	93.14(4)	N(8)	O(10)	K(2)	87.36(11)
O(5)	K(1)	O(1)	99.35(4)	N(8)	O(9)	K(2)	102.28(11)
O(5)	K(1)	N(1)	122.34(4)	N(7)	O(5)	K(1)	127.20(12)
O(5)	K(1)	N(4)	68.85(4)	N(7)	O(6)	K(2)	132.19(12)
O(5)	K(1)	N(2)	136.90(5)	O(2)	N(1)	K(1)	55.64(9)
N(1)	K(1)	K(2)	52.86(3)	O(2)	N(1)	N(2)	123.09(15)
N(1)	K(1)	K(2)	57.62(3)	O(1)	N(1)	K(1)	68.97(9)
N(4)	K(1)	K(2)	138.02(3)	O(1)	N(1)	O(2)	119.05(15)
N(4)	K(1)	K(2)	86.72(3)	O(1)	N(1)	N(2)	117.83(15)
N(4)	K(1)	O(4)	54.40(4)	N(2)	N(1)	K(1)	157.74(12)
N(4)	K(1)	O(1)	132.60(4)	O(8)	N(6)	C(4)	121.29(16)
N(4)	K(1)	N(1)	137.60(4)	O(7)	N(6)	O(8)	121.63(15)
N(4)	K(1)	N(2)	78.85(4)	O(7)	N(6)	C(4)	117.08(16)
N(2)	K(1)	K(2)	62.80(3)	N(5)	N(4)	K(1)	129.26(11)
N(2)	K(1)	K(2)	143.03(3)	C(1)	N(4)	K(1)	125.21(12)
N(2)	K(1)	N(1)	100.74(4)	C(1)	N(4)	N(5)	105.29(15)
K(1)	K(2)	K(1)	98.499(11)	N(1)	N(2)	K(1)	108.38(10)
O(2)	K(2)	K(1)	39.30(3)	N(1)	N(2)	C(3)	112.71(14)
O(2)	K(2)	K(1)	130.01(3)	C(3)	N(2)	K(1)	131.13(12)
O(2)	K(2)	O(8)	140.34(5)	N(4)	N(5)	C(4)	118.41(15)
O(2)	K(2)	O(4)	75.41(4)	N(4)	N(5)	C(2)	110.21(15)
O(2)	K(2)	O(1)	92.26(4)	C(2)	N(5)	C(4)	131.03(16)

O(2)	K(2)	O(10)	137.99(4)		O(5)	N(7)	C(4)	115.86(16)
O(2)	K(2)	O(9)	147.32(4)		O(6)	N(7)	O(5)	122.65(16)
O(2)	K(2)	O(6)	85.34(4)		O(6)	N(7)	C(4)	121.48(16)
O(2)	K(2)	N(8)	152.23(4)		O(10)	N(8)	K(2)	71.13(10)
O(8)	K(2)	K(1)	37.06(3)		O(10)	N(8)	O(9)	123.55(16)
O(8)	K(2)	K(1)	129.41(3)		O(10)	N(8)	C(2)	117.80(16)
O(8)	K(2)	O(4)	125.74(4)		O(9)	N(8)	K(2)	56.67(9)
O(8)	K(2)	O(10)	62.32(4)		O(9)	N(8)	C(2)	118.65(15)
O(8)	K(2)	O(9)	72.26(4)		C(2)	N(8)	K(2)	156.87(12)
O(8)	K(2)	N(8)	61.55(4)		O(4)	N(3)	C(1)	117.97(16)
O(4)	K(2)	K(1)	90.09(3)		O(3)	N(3)	O(4)	124.38(17)
O(4)	K(2)	K(1)	45.14(3)		O(3)	N(3)	C(1)	117.62(16)
O(4)	K(2)	O(10)	124.76(4)		N(4)	C(1)	N(3)	116.90(16)
O(4)	K(2)	N(8)	106.28(4)		N(4)	C(1)	C(3)	114.00(17)
O(1)	K(2)	K(1)	57.53(3)		C(3)	C(1)	N(3)	129.05(17)
O(1)	K(2)	K(1)	40.98(3)		N(2)	C(3)	C(1)	132.21(18)
O(1)	K(2)	O(8)	75.16(4)		C(2)	C(3)	N(2)	126.48(17)
O(1)	K(2)	O(4)	61.65(4)		C(2)	C(3)	C(1)	101.23(16)
O(1)	K(2)	O(10)	129.47(4)		N(6)	C(4)	N(5)	117.85(16)
O(1)	K(2)	O(9)	101.62(4)		N(6)	C(4)	N(7)	124.51(17)
O(1)	K(2)	O(6)	90.51(4)		N(7)	C(4)	N(5)	116.77(16)
O(1)	K(2)	N(8)	113.23(4)		N(5)	C(2)	N(8)	121.30(17)
O(7)	K(2)	K(1)	106.66(3)		N(5)	C(2)	C(3)	109.23(16)
O(7)	K(2)	K(1)	154.66(4)		C(3)	C(2)	N(8)	129.42(17)
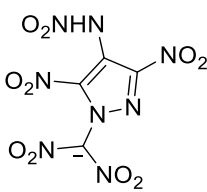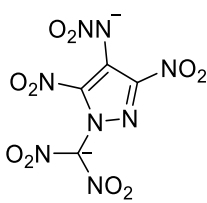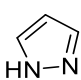
Table S4. Torsion Angles for **6**

A	B	C	D	Angle/°	A	B	C	D	Angle/°
K1	O2	N1	O1	-28.70(11)	K24	O9	N8	C2	153.50(10)
K1	O2	N1	N2	153.20(10)	K28	O6	N7	O5	-151.3(15)
K11	O8	N6	O7	-52.28(15)	K28	O6	N7	C4	27.80(18)
K11	O8	N6	C4	127.96(14)	K24	N8	C2	N5	69.0(3)
K12	O4	N3	O3	-156.6(14)	K24	N8	C2	C3	-108.2(3)
K12	O4	N3	C1	21.32(14)	O2	N1	N2	C3	-9.28(19)
K1	O1	N1	O2	25.14(10)	O8	N6	C4	N5	-176.2(16)
K1	O1	N1	N2	-156.67(9)	O8	N6	C4	N7	-7.3(2)
K13	O10	N8	K24	-173.9(3)	O4	N3	C1	N4	-19.90(18)
K13	O10	N8	O9	-151.3(3)	O4	N3	C1	C3	162.92(16)
K13	O10	N8	C2	29.4(3)	O1	N1	N2	C3	172.61(17)
K15	O5	N7	O6	-23.59(16)	O7	N6	C4	N5	4.02(18)
K15	O5	N7	C4	157.24(14)	O7	N6	C4	N7	172.95(15)
K1	N1	O2	K26	121.73(10)	O10	N8	C2	N5	176.72(16)
K1	N1	O1	K27	105.74(7)	O10	N8	C2	C3	-0.5(2)
K1	N1	N2	K13	-137.1(3)	O9	N8	C2	N5	-2.59(19)
K1	N1	N2	C3	70.0(3)	O9	N8	C2	C3	-179.83(16)

K12	N4	N5	C4	0.13(15)	O5	N7	C4	N6	-160.6(15)
K12	N4	N5	C2	174.07(15)	O5	N7	C4	N5	8.42(18)
K12	N4	C1	N3	8.96(14)	O6	N7	C4	N6	20.2(2)
K12	N4	C1	C3	-173.4(14)	O6	N7	C4	N5	-170.8(18)
K13	N2	N1	K1	-137.1(15)	N1	N2	C3	C1	-46.6(2)
K13	N2	N1	O2	143.67(10)	N1	N2	C3	C2	137.01(16)
K13	N2	N1	O1	-34.45(12)	N6	C4	N5	N4	-89.84(18)
K13	N2	C3	C1	168.35(15)	N6	C4	N5	C2	97.70(19)
K13	N2	C3	C2	-8.02(17)	O3	N3	C1	N4	158.13(17)
K26	O2	N1	O1	93.03(16)	O3	N3	C1	C3	-19.1(2)
K26	O2	N1	N2	-85.07(17)	N4	N5	C4	N7	100.37(17)
K28	O8	N6	O7	128.93(13)	N4	N5	C2	N8	-178.4(14)
K28	O8	N6	C4	-50.83(15)	N4	N5	C2	C3	-0.64(16)
K29	O4	N3	O3	-54.13(14)	N4	C1	C3	N2	-178.7(14)
K29	O4	N3	C1	123.76(11)	N4	C1	C3	C2	-1.70(17)
K27	O1	N1	O2	130.88(14)	N2	C3	C1	N3	-1.5(3)
K27	O1	N1	N2	-50.92(15)	N2	C3	C2	N5	178.6(2)
K2	O7	N6	O8	90.8(2)	N2	C3	C2	N8	-3.9(2)
K2	O7	N6	C4	-89.4(3)	N5	C2	C3	C1	1.32(16)
K24	O10	N8	O9	22.57(12)	N8	C2	C3	C1	178.8(2)

3.Guassian calculation

Scheme S1. Isodesmic reactions of target compounds.

Table S5. Ab Initio computational data.

Specis	E_0[a] /Hatree	H_{corr}[b] / Hatree	ZPE[c] / Hatree	ΔH_f[d] / Hatree
O₂NHN, NO₂, O₂N, N–N, O₂N, NO₂	-1340.4226	0.134116	0,011458	-151.9535387
O₂NN⁻, NO₂, O₂N, N–N, O₂N, NO₂	-1339.8123	0.120089	0.100826	-38.5654
CH₄	-40.39849	0.048605	0.044793	-74.6
NH3	-56.43418	0.03819	0.034372	-45.9
HN–N	-225.7181	0.075955	0.071265	105.4
CH₃NO₂	-244.5544	0.055129	0.049856	-74.3
CH₃NH₂	-95.63188	0.068401	0.064032	-23
⁻NHNO₂	-260.012	0.03044	0.026167	-84
⁻CHC(NO₂)₂	-448.1641	0.046605	0.039726	-233
NH₂NO₂	-260.5479	0.042613	0.039257	-6.1
K⁺	–	–	–	501.1[3]

[a] Total energy (E_0) calculated by MP2/6-311++G**//B3LYP/6-31+G** method; [b] Values of thermal correction (H_{corr}); [c] Zero-point energy correction (ZPE); [d] Heat of formation (ΔH_f).

Heat of formation

Calculations were carried out by using the Gaussian 09 (Revision E.01) suite of programs.[4] The geometric optimization of the structures and frequency analyses were carried out by using the B3LYP functional with the 6-31+G**basis set, and single-point

energies were calculated at the MP2(full)/6-311++G**level. All of the optimized structures were characterized to be true local energy minima on the potential-energy surface without imaginary frequencies.
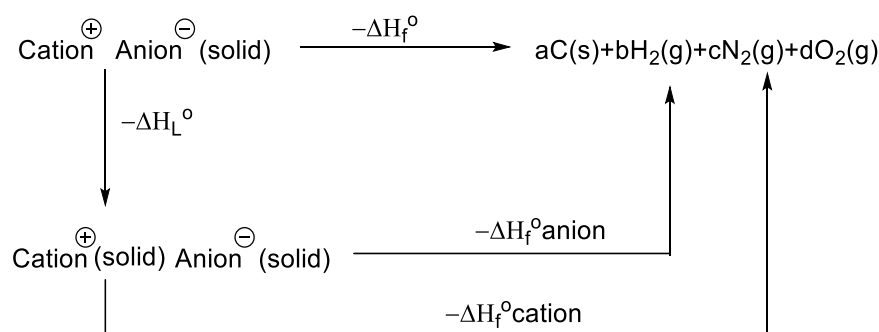
Figure S2. Born-Haber cycle for the formation for energetic salts.

Based on the Born-Haber energy cycle (Figure S20), the heat of formation of a salt can be simplified according to Equation (1), where $\triangle HL$ is the lattice energy of the salt.

$$\triangle H_f^o(\text{ionic salt, 298K}) = \triangle H_f^o (\text{cation, 298K}) + \triangle H_f^o (\text{anion, 298K}) - \triangle H_L \quad (1)$$

The $\triangle H_L$ value could be predicted by the formula suggested by Jenkins et al [Eq. (2)][i], where U_{POT} is the lattice potential energy and n_M and n_X depend on the nature of the ions M^{p+} and X^{q-}, respectively, and are equal to three for monoatomic ions, five for linear polyatomic ions, and six for nonlinear polyatomic ions.

$$\triangle H_L = U_{POT} + [p(n_M/2-2) + q(n_X/2-2)]RT \quad (2)^{[5]}$$

The equation for the lattice potential energy, U_{POT}, takes the form of Equation (3), where ρ_m is the density (g cm^{-3}), Mm is the chemical formula mass of the ionic material (g), and the coefficients γ (kJ^{-1}mol^{-1}cm) and δ (kJ^{-1}mol^{-1}) are assigned literature values (2:1 salts γ=8375.6, δ=-178.8; 1:1 salts γ=1981.2 δ=103.8)[6].

$$U_{POT} \text{ (kJ}^{-1}\text{mol}^{-1}) = \gamma (\rho_m/Mm)^{1/3} + \delta \quad (3)$$

Table S6. Calculated heat of formation for **6** and **8·2H₂O**.

Compound	ΔH_L (KJ/mol)	ΔH_f^{cation} (KJ/mol)	ΔH_f^{Anion} (KJ/mol)	ΔH_f^{298K} (KJ/mol)
6	1279.3	501.1	-38.6	-315.7
8·2H₂O	1242.5	501.1	-152.0	-893.3

Detonation performances calculation

Detonation pressure (*P*) and detonation velocity (*D*) were calculation according to the Kamlet-Jacobs equations[6].

$$D = 1.01\left(N\overline{M}^{1/2}Q^{1/2}\right)^{1/2}(1 + 1.30\rho \quad (4)$$

$$P = 1.558\rho^2\overline{M}^{1/2}Q^{1/2} \quad (5)$$

where each term in eqs 4 and 5 is defined as follows: D, the detonation velocity (km s^{-1}); P, the detonation pressure (GPa); N, the moles of detonation gases per gram explosive; M the average molecular weight of these gases (g mol^{-1}); Q, the heat of

detonation[6a] (cal g^{-1}); and ρ, the loaded density of explosives (g cm^{-3}). The density calculated by single crystal X-ray diffractometer at low temperature were ture to density at 298K by the volume expansion equation (6).

$$\rho = \frac{\rho T}{(1+\alpha v(298-T))}; \quad \alpha v = 1.5 \times 10^{-4} K^{-1} \tag{6}$$
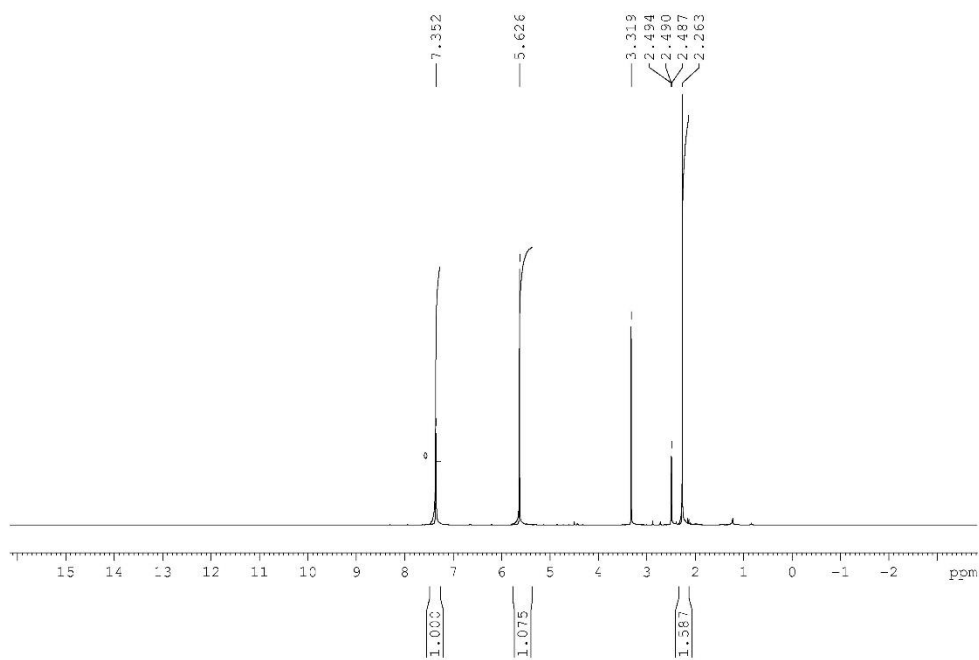
4. NMR Spectrum of the prepared compounds

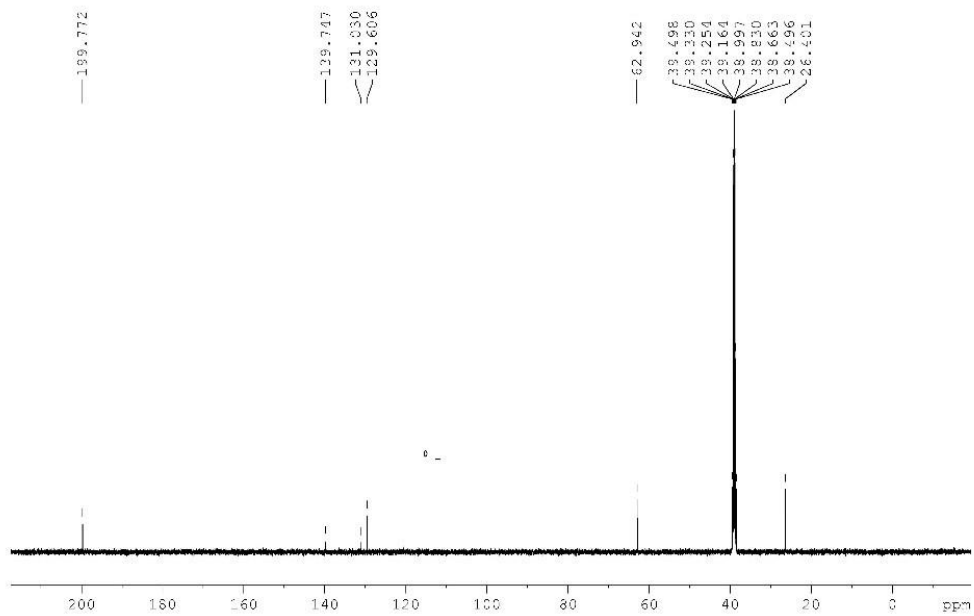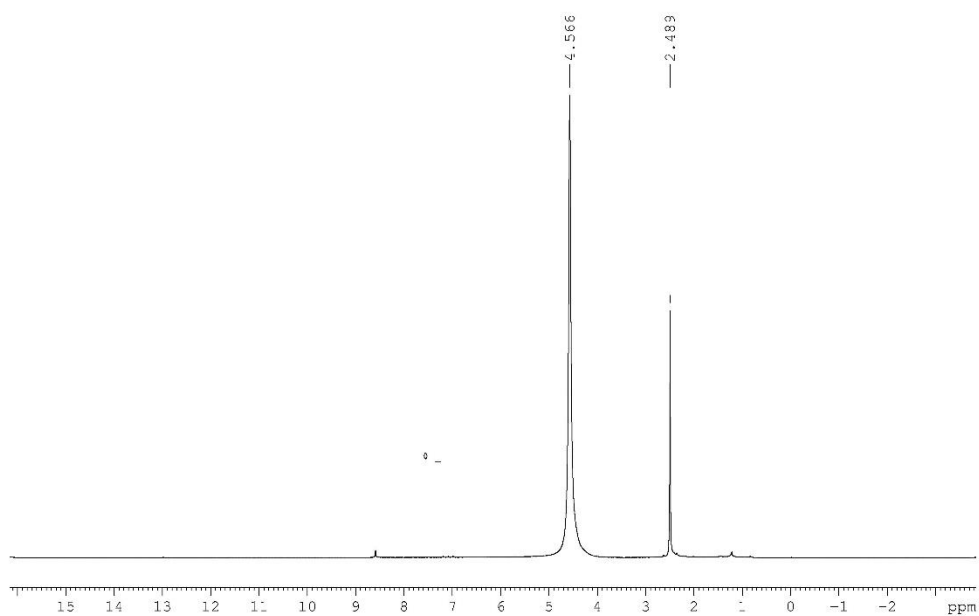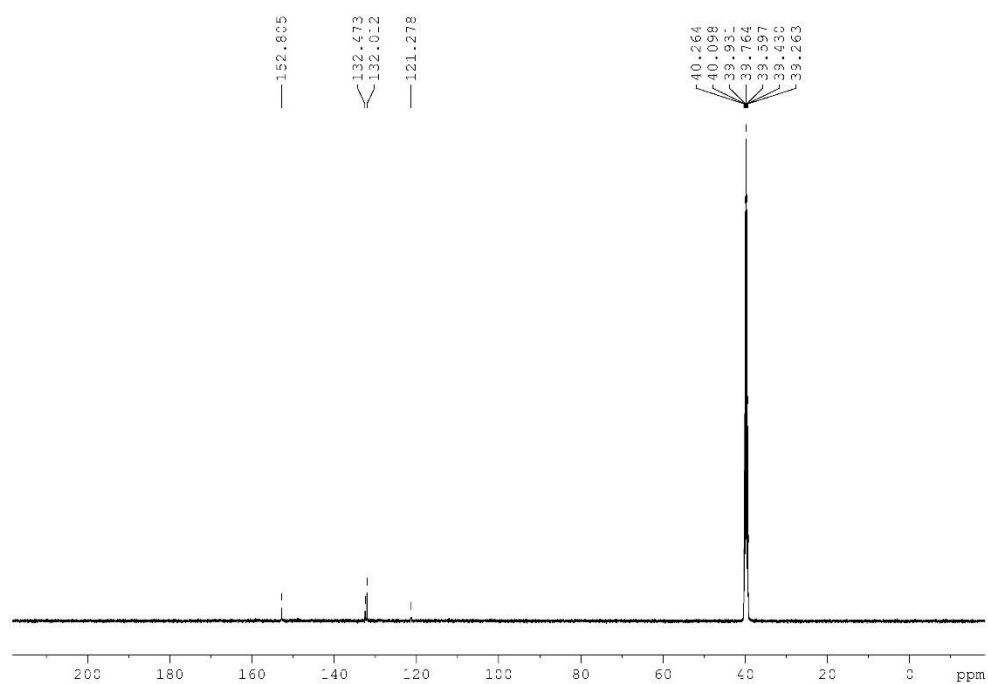**Figure S3.** ^{1}H NMR spectrum of compound **4**.

Figure S4. ^{13}C NMR spectrum of compound **4**.

Figure S5. ^{1}H NMR spectrum of compound **5**.

Figure S6. ^{13}C NMR spectrum of compound **5**.

149.26
135.10
132.71
127.94
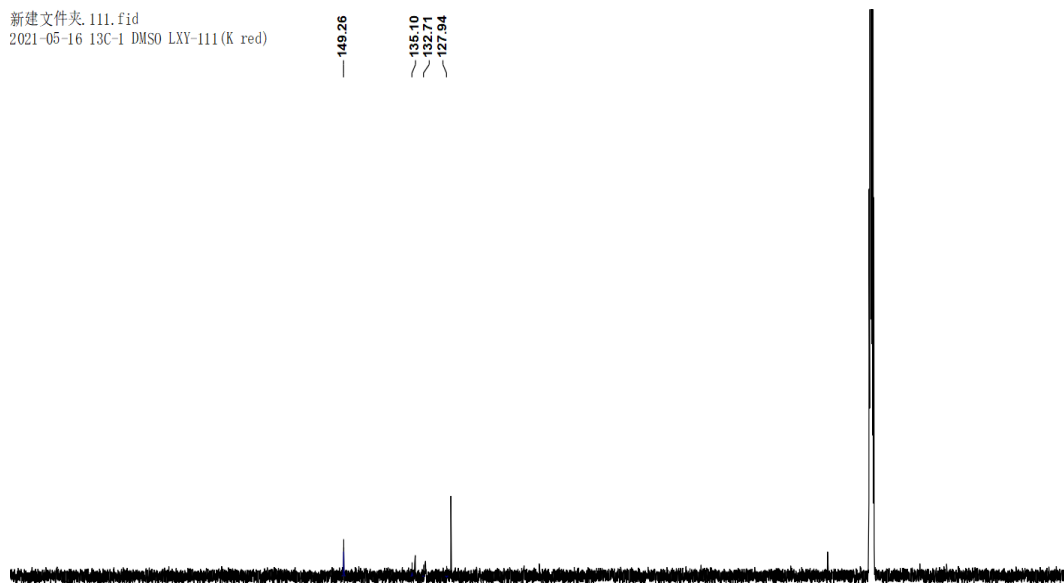
Figure S7. ^{13}C NMR spectrum of compound **6**.

5.065
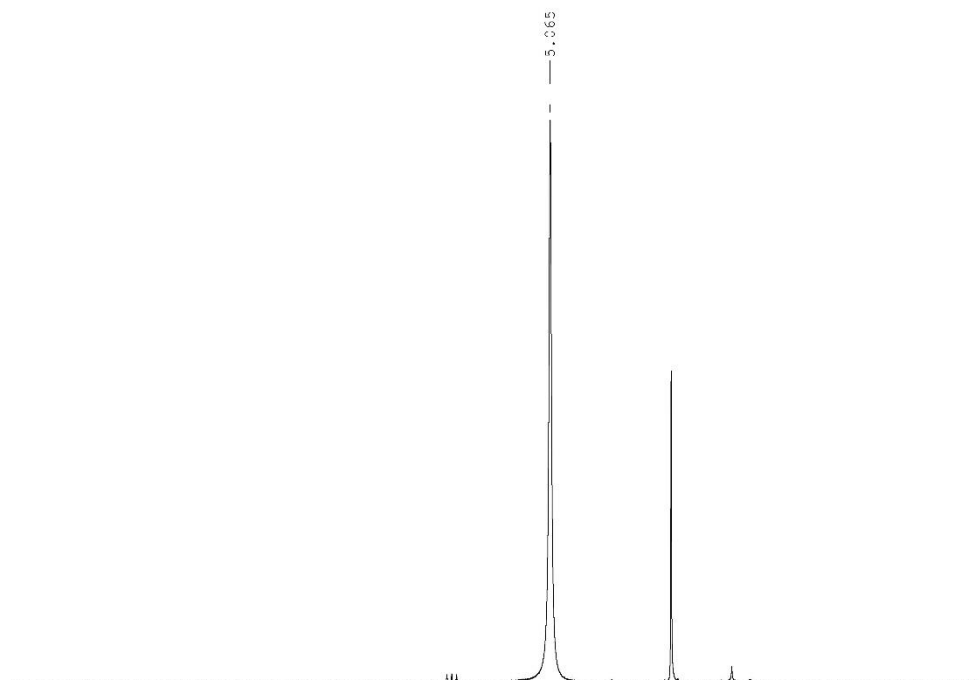
Figure S8. ^{1}H NMR spectrum of compound **8**·2H$_2$O.
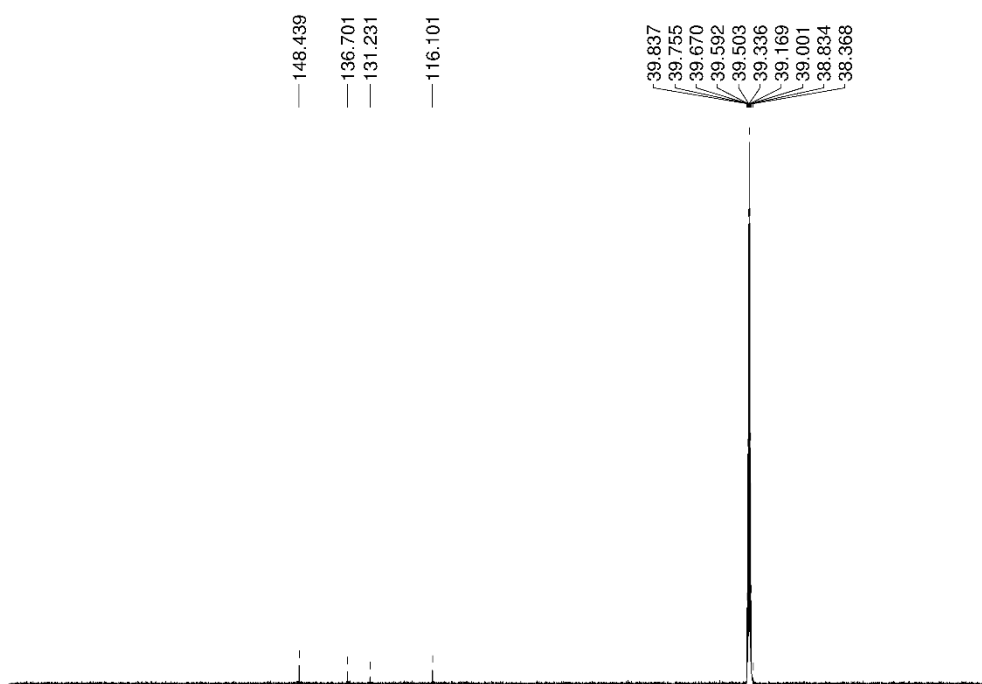
Figure S9. ^{13}C NMR spectrum of compound **8**·2H$_2$O.

5. Mass spectrometry of compound 5 and 8·2H$_2$O.
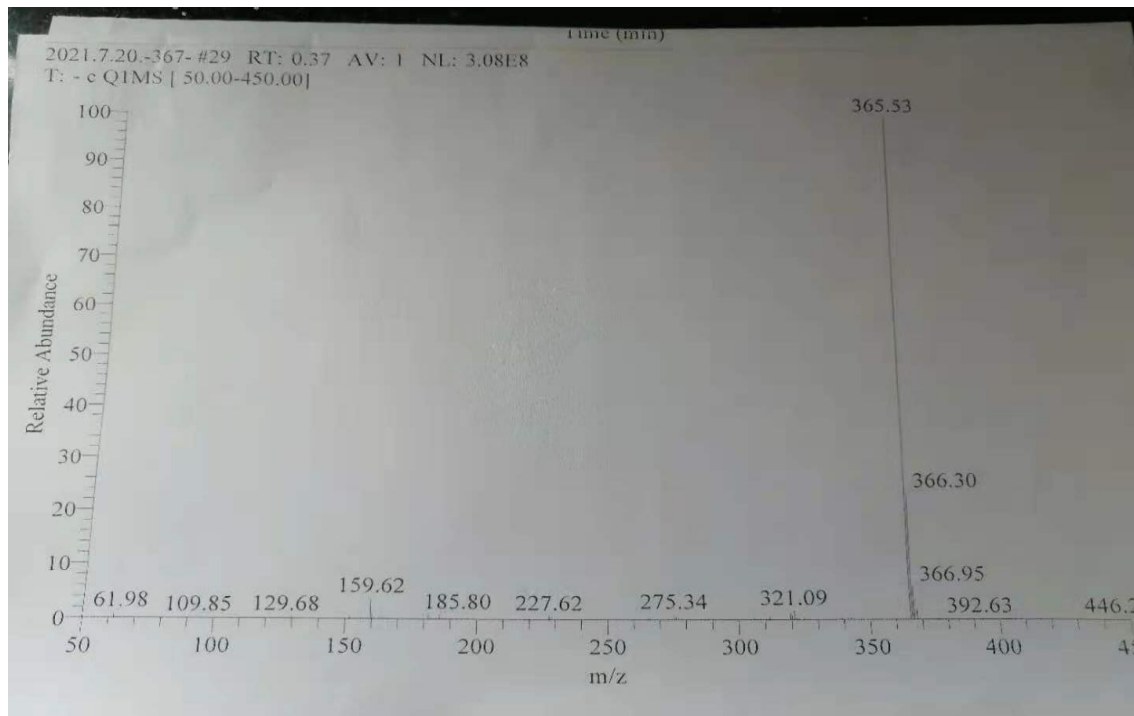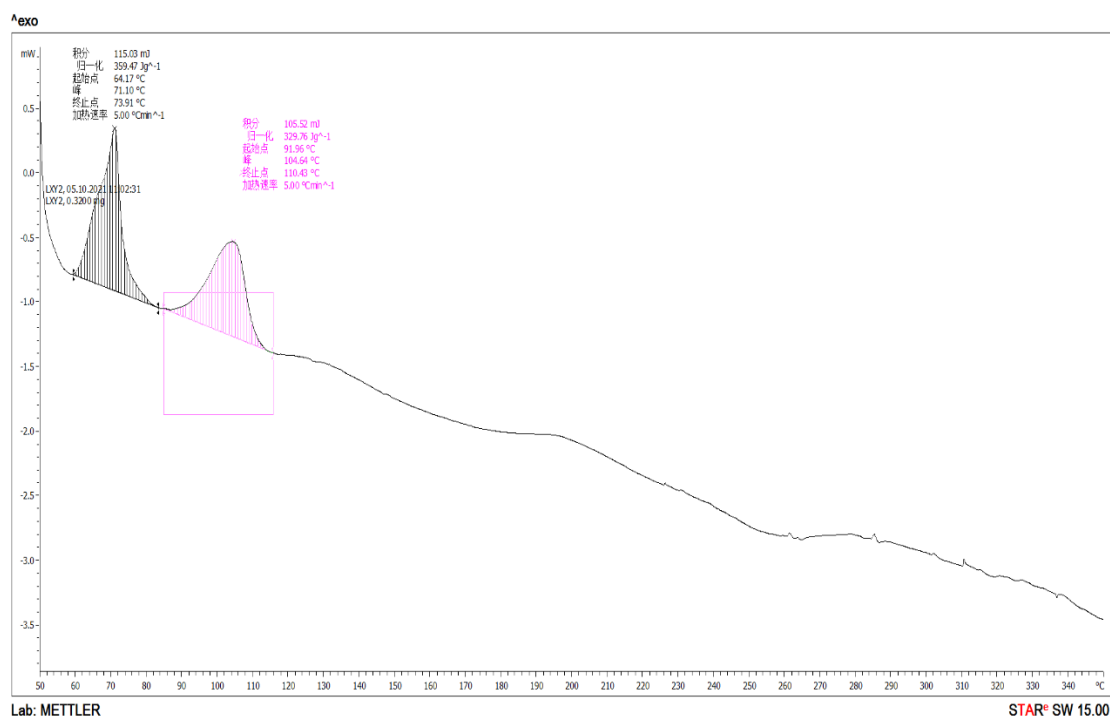

Figure S10. The mass spectrum of compound **5**.
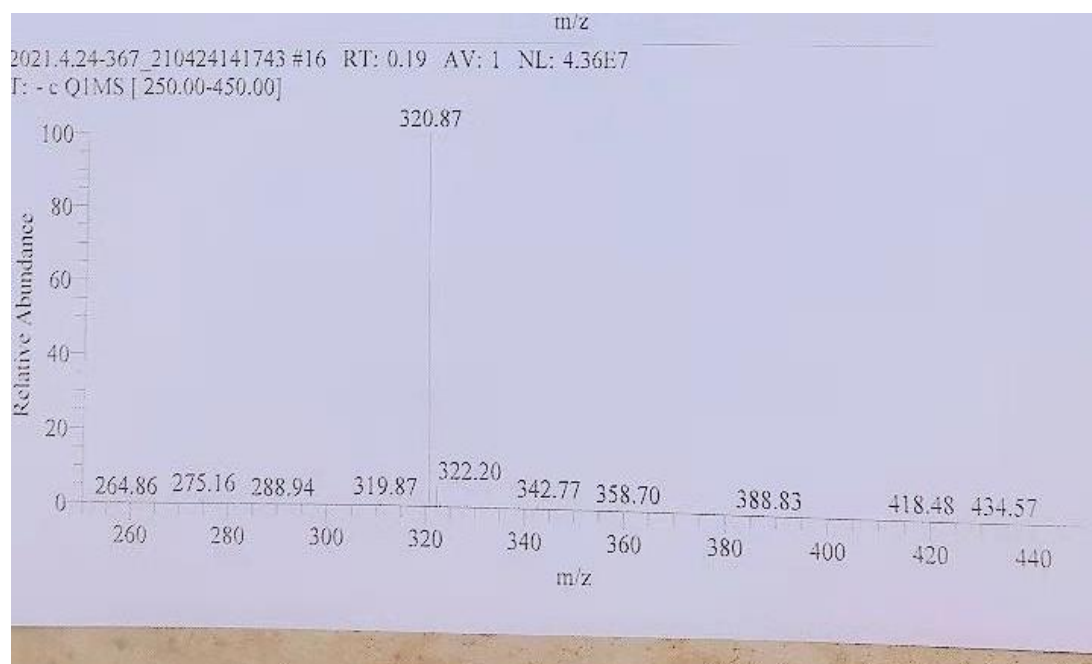
Figure S11. The mass spectrum of compound **8**·2H$_2$O.

6. DSC curves of compounds 6 and 8·2H$_2$O.
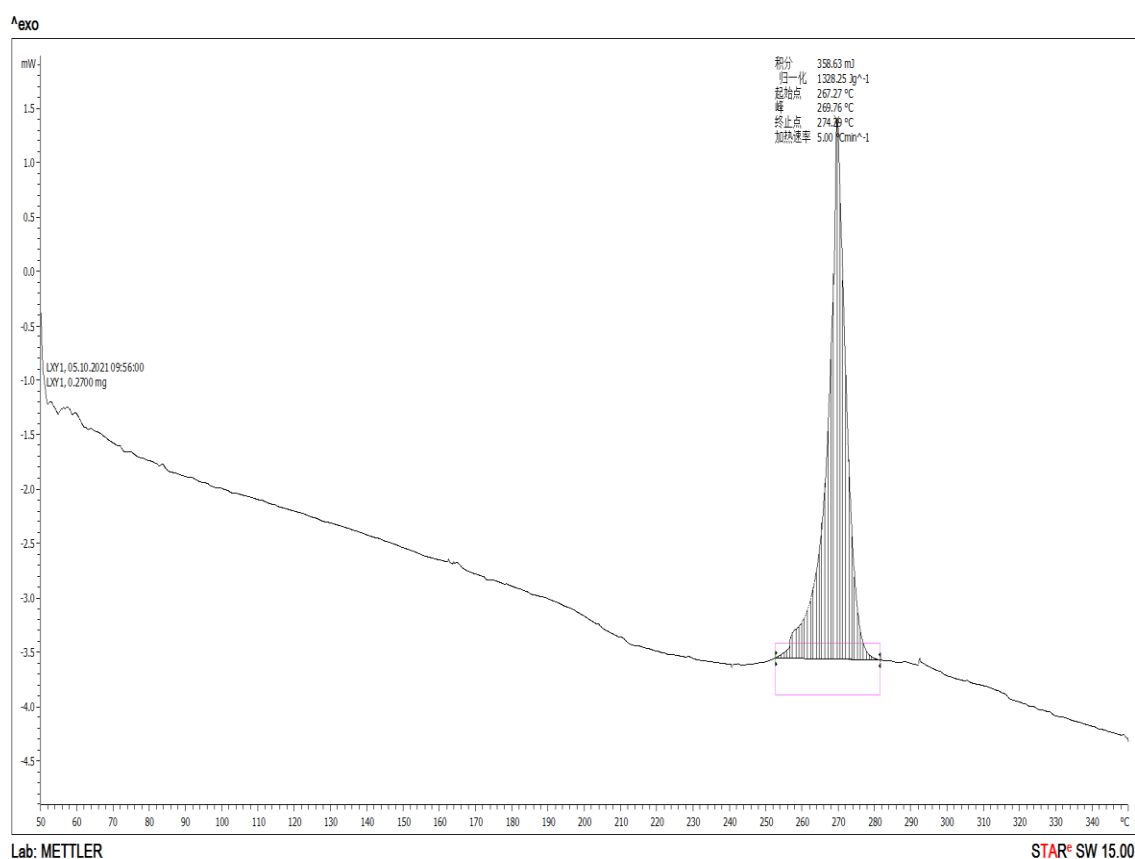
Figure S12. The DSC curves of compound **6**.

Figure S13. The DSC curves of compound **8**·2H$_2$O.

[1] G. M. Sheldrick, SADABS: Area Detector Absorption Correction; University of Göttingen:Göttingen, Germany, 2001.

[2] Sheldrick, G. M. *SHELXT*–Integrated space-group and crystal structure Determination. *Acta Cryst.* **2015**, *A71*, 3-8.

[3] H. Gao, C. Ye, C. M. Piekarski, J. M. Shreeve, *J. Phys. Chem. C* **2007**, *111*, 10718 −10731.

[4] Revision A.01, Gaussian, Inc. Wallingford CT, **2009**.

[5] H. D. B. Jenkins. *Inorg.Chem*. **2002**, 41, 2364–2367

[6] (a) M. J. Kamlet, S. J. Jacobs. *J. Chem. Phys*. **1968**, *48*, 23-35; (b) M. J. Kamlet, J. E. Ablard. *J. Chem. Phys*. **1968**, *48*, 36-42; (c) M. J. Kamlet, C. Dicknison. *J. Chem. Phys*. **1968**, *48*, 43-49. (d) H. Gao, C. Ye, C. Piekarski, J. M. Shreeve. *J. Phys. Chem. C*. **2007**, 111, 10718-10731.